

- improving the pharmacokinetics of ¹⁸⁶Re-MAG3-conjugated bisphosphonate (¹⁸⁶Re-MAG3-HBP), an agent for treatment of painful bone metastases. *Eur J Nucl Med Mol Imaging* 2009, **36**(1):115–121.
15. Thomas DM, Zalberg JR: 5-fluorouracil: a pharmacological paradigm in the use of cytotoxics. *Clin Exp Pharmacol Physiol* 1998, **25**(11):887–895.
 16. Cao S, Rustum YM: Synergistic antitumor activity of irinotecan in combination with 5-fluorouracil in rats bearing advanced colorectal cancer: role of drug sequence and dose. *Cancer Res* 2000, **60**(14):3717–3721.
 17. Salonga D, Danenberg KD, Johnson M, Metzger R, Groshen S, Tsao-Wei DD, Lenz HJ, Leichman CG, Leichman L, Diasio RB, *et al*: Colorectal tumors responding to 5-fluorouracil have low gene expression levels of dihydropyrimidine dehydrogenase, thymidylate synthase, and thymidine phosphorylase. *Clin Cancer Res* 2000, **6**(4):1322–1327.

doi:10.1186/1471-2407-12-448

Cite this article as: Yoshimi *et al.*: Use of a chemically induced-colon carcinogenesis-prone *Apc*-mutant rat in a chemotherapeutic bioassay. *BMC Cancer* 2012 **12**:448.

**Submit your next manuscript to BioMed Central
and take full advantage of:**

- Convenient online submission
- Thorough peer review
- No space constraints or color figure charges
- Immediate publication on acceptance
- Inclusion in PubMed, CAS, Scopus and Google Scholar
- Research which is freely available for redistribution

Submit your manuscript at
www.biomedcentral.com/submit





GASTROINTESTINAL, HEPATOBILIARY, AND PANCREATIC PATHOLOGY

Tumor Suppressor APC Protein Is Essential in Mucosal Repair from Colonic Inflammation through Angiogenesis

Kazuto Yoshimi,* Takuji Tanaka,[†] Tadao Serikawa,* and Takashi Kuramoto*

From the Institute of Laboratory Animals,* Graduate School of Medicine, Kyoto University, Kyoto; and Cancer Research and Prevention,[†] The Tohoku Cytopathology Institute, Gifu, Japan

Accepted for publication
December 24, 2012.

Address correspondence to
Takashi Kuramoto, Ph.D.,
Institute of Laboratory Animals,
Graduate School of Medicine,
Kyoto University,
Yoshidakonoe-cho,
Sakyo-ku, Kyoto 606-8501,
Japan. E-mail: tkuramot@
anim.med.kyoto-u.ac.jp.

Mucosal repair after acute colonic inflammation is central to maintaining mucosal homeostasis. Failure of mucosal repair often leads to chronic inflammation, sometimes associated with inflammatory bowel disease (IBD). The adenomatous polyposis coli (*APC*) tumor suppressor gene regulates the Wnt signaling pathway, which is essential for epithelial development, and inactivation of *APC* facilitates colorectal cancer. Our previous study suggested that *APC* is involved in pathogenesis of colonic inflammation; however, its role in mucosal repair remains unknown. In this article, we report that colitis induced by dextran sodium sulfate persisted with delayed mucosal repair in Kyoto Apc Delta (KAD) rats lacking the APC C terminus. Defects in the repair process were accompanied by an absence of a fibrin layer covering damaged mucosa and reduced microvessel angiogenesis. APC was up-regulated in vascular endothelial cells (VECs) in inflamed mucosa in KAD and F344 (control) rats. The VECs of KAD rats revealed elevated cell adhesion and low-branched and short-length tube formation. We also found that DLG5, which is associated with IBD pathogenesis, was up-regulated in VECs in inflamed mucosa and interacted with the C terminus of APC. This finding suggests that loss of interaction between the APC C terminus and DLG5 affects VEC morphology and function and leads to persistence of colitis. Therefore, APC is essential for maintenance of intestinal mucosal homeostasis and can consequently contribute to IBD pathogenesis. (*Am J Pathol* 2013, 182: 1263–1274; <http://dx.doi.org/10.1016/j.ajpath.2012.12.005>)

Mucosal epithelial defense is an important system to prevent injuries induced by undigested substances, acid, ischemia, and microbial infection.^{1,2} Once the mucosa is injured, the repair process—which is complex but primarily consists of the immune response, granulation tissue formation, angiogenesis, and epithelial regeneration—plays a central role to prevent further injuries.³ Defects in such repair systems are a potential risk for persistent inflammation of the intestine or colon, which can lead to chronic inflammation, such as that seen in inflammatory bowel disease (IBD).

IBD, including ulcerative colitis and Crohn's disease, represents a chronic, relapsing and remitting inflammatory condition that affects individuals throughout life.⁴ Patients with IBD are at risk of developing colorectal cancer.⁵ Although it is widely accepted that genetic, environmental, and immunologic factors are involved,^{6,7} the pathogenesis of IBD remains unclear. No completely effective therapeutic strategy has yet been established.

To investigate the pathogenesis of IBD, animal models of experimental colitis have been developed.⁸ The dextran sodium sulfate (DSS) model is excellent for its resemblance to the clinical symptom of the IBD and for its ease of reproducibility and accessibility.⁹ Providing drinking water containing DSS for several days induces colitis in rodents, which has characteristics similar to human ulcerative colitis, such as signs of diarrhea, gross rectal bleeding, weight loss, shortening of the colorectum, histologic features of multiple erosions, and inflammatory mucosal changes, occasionally including crypt abscess. Colitis is also predominant in the

Supported in part by a Grant-in-Aid for Cancer Research from the Ministry of Health, Labour and Welfare and Grants-in-Aid for Scientific Research from the Japan Society for the Promotion of Science (21300153 to T.K. and 0233639 to K.Y.).

The KAD (F344-*Apc*^{m1Ky0}) rat has been deposited in the National Bio-resource Project-Rat in Japan (Institute of Laboratory Animals, Kyoto University).

descending and sigmoid colons and the rectum and associated with alteration of intestinal flora. Some pathogenic and regulatory factors demonstrated in the DSS model, such as cytokines, growth factors, and inflammatory enzymes, have been exploited to develop future therapeutic strategies against IBD.⁸

Adenomatous polyposis coli (*APC*) has been identified as the causative gene of familial adenomatous polyposis of the colon, which is characterized by numerous polyps in the intestine.¹⁰ Genetic studies using mutant mouse models indicate that *APC* is essential for development and that its inactivation facilitates tumorigenesis.¹¹

APC is a 2843–amino acid polypeptide and is composed of multiple domains. Via these domains, *APC* can bind to various proteins, including the guanine-nucleotide-exchange factor ASEF1, the Wnt pathway component β -catenin, microtubules (MTs), the cytoskeletal regulator EB1, and homologs of the *Drosophila* disks large protein (DLG).¹² Most cancer-linked *APC* mutations occur at the central region of *APC* (the so-called mutation cluster region) and result in truncation of almost half of the C terminal region of the protein.¹³ Because these truncations cause loss of the domains required for binding to β -catenin, MTs, EB1, and DLG, the interaction of *APC* with these molecules has been considered essential for its tumor-suppressing activity.

In 1999, Smits et al¹⁴ developed a knockout mouse that carried a targeted mutation at codon 1638, *Apc*^{1638T} (T for truncated). The resultant truncated *APC* protein contains β -catenin binding sites but lacks all of the C-terminus domains. *Apc*^{1638T/1638T} mice survive to adulthood and are tumor free. Thus, the interaction of *APC* with β -catenin but not MTs, EB1, or DLG is critical in tumorigenesis. In addition, *Apc*^{1638T/1638T} mice have growth retardation, reduced postnatal viability, the absence of preputial glands, and the formation of nipple-associated cysts.¹⁴ Enlarged thyroid follicles and low responsiveness to thyroid-stimulating hormone are also found with *Apc*^{1638T/1638T} mice.¹⁵ Therefore, the C terminus of *APC* appears to be involved in the development of several tissues as described in this article; however, its physiologic function *in vivo* remains unclear.

We recently developed a mutant rat that carries a homozygous nonsense mutation at codon 2523 (*Apc*^{A2523}), which we call the Kyoto *Apc* Delta (KAD) rat.¹⁶ The KAD rat expresses truncated *APC* protein that contains β -catenin binding sites but lacks the C terminus (321 amino acids in length), which can bind to MT, EB1, and DLG. KAD rats survive to adulthood and are free of intestinal tumors. However, when KAD rats received a single subcutaneous administration of 20 mg/kg of azoxymethane and 1 week later were given 2% DSS (in drinking water) for 1 week, they had a significantly higher incidence and multiplicity of colon tumors at week 15 compared with control F344 rats.^{16,17} In contrast, KAD rats treated with azoxymethane only did not develop colon tumors (as assessed by the carcinogenesis test) by 15 weeks, similar to the azoxymethane-treated F344 rats. These findings suggest that the KAD rat is susceptible to

inflammation provoked by the colitis-inducing agent and that the C terminus of *APC* appears to be involved in the pathogenesis of colitis.

In this study, we found that loss of the C terminus of *APC* affected the morphology and function of vascular endothelial cells (VECs) and led to a persistence of colitis. Our results reveal a new role of *APC* in the angiogenesis associated with mucosal repair of damage due to colitis.

Materials and Methods

Rats

F344/NSlc and KAD (homozygous for the *Apc*^{A2523} mutation, official strain name: F344-*Apc*^{m1Ky0}) rats were obtained from Japan SLC, Inc. (Hamamatsu, Japan). KAD rats were backcrossed five times with female F344/NSlc rats to remove latent mutations induced by N-ethyl N-nitrosourea.¹⁶ The rats were kept at the Institute of Laboratory Animals, Graduate School of Medicine, Kyoto University, under conditions of 50% humidity and a 14:10-hour light:dark cycle. They were fed a standard pellet diet (F-2, Oriental Yeast Co., Ltd, Tokyo, Japan) and tap water *ad libitum*.

Induction of Colitis

Male KAD rats ($n = 30$) and control F344/NSlc rats (F344 rats, $n = 30$) aged 5 weeks were given 2% DSS (molecular weight = 36,000–50,000 kDa) (MP Biochemicals, LLC., Solon, OH) in their drinking water for 1 week. The rats were divided into three groups: those sacrificed immediately after DSS treatment (week 1), those sacrificed 1 week after terminating the treatment (week 2), and those sacrificed 3 weeks after the treatment (week 4). The animals were sacrificed by cervical dislocation under anesthesia with isoflurane (Mylan Inc., New York, NY). The experimental procedures were approved by the Animal Research Committee of Kyoto University and were performed according to the Regulations on Animal Experimentation of Kyoto University.

Clinical assessment of inflammation involved monitoring the body weight and scoring the diarrhea and fecal blood for each rat.¹⁸ The presence of diarrhea and fecal blood were scored on a scale of 1 and 2, respectively. The clinical inflammatory score for each animal was obtained by adding the diarrhea and fecal blood scores.

Histopathologic Analysis

An hour prior to sacrifice, the rats were injected intraperitoneally with 50 mg/kg of 5-bromo-2'-deoxyuridine (BrdU; Sigma, St. Louis, MO) to permit immunohistochemical (IHC) analysis of BrdU. On autopsy, the colorectum of each rat was resected and gently washed with PBS to remove feces. Half was used for a RT-PCR assay, and the other was fixed in 10% buffered formalin and embedded in paraffin for histopathologic analysis. Five serial sections of colonic

tissues (3 μm thick) were made: two sections stained with H&E to permit histologic examination and with phosphotungstic acid hematoxylin (PTAH) for detection of fibrin. Other sections were used for IHC with an LSAB2 Kit (Dako, Glostrup, Denmark). Anti-APC monoclonal antibody (EP701Y; Abcam, Cambridge, UK) and anti-CD31/platelet-endothelial cell adhesion molecule 1 polyclonal antibody (Santa Cruz Biotechnology, Santa Cruz, CA) were used as primary antibodies.

Cell proliferation in the inflamed mucosa was accessed by determination of the labeling index for BrdU-positive cells. The number of BrdU-positive cells was counted in at least 20 well-oriented crypts for each group. The labeling index was calculated by dividing the number of BrdU-positive cells by the total number of nucleated cells for each well-oriented crypt.

To investigate the localization of EB1, DLG1, and DLG5 in the inflamed colon, fluorescent immunocytochemistry was performed. Anti-CD31 polyclonal antibody (Santa Cruz Biotechnology) and anti-EB1, anti-DLG1, and anti-DLG5 polyclonal antibodies (Abcam) were used as primary antibodies. Alexa Fluor 488-conjugated anti-rabbit IgG antibody and Alexa Fluor 594-conjugated anti-mouse IgG antibody (1:200; Invitrogen, Carlsbad, CA) were used as secondary antibodies. Immunostained sections were visualized using a Bioevo immunofluorescence microscope (Keyence, Osaka, Japan).

Analysis of Colonic Microvasculature Density

Vascular density was calculated using an international consensus method to quantify angiogenesis, as previously described.¹⁹ Briefly, CD31-stained distal colonic sections were scanned and the number of vessels within the mucosa was counted to identify the most vascularized area. Vascular density per field was obtained from at least five microphotographs of the most vascularized mucosa for each rat. Quantitative analysis of the data was performed using WinROOF software version 6.0 (Mitani Corp., Fukui, Fukui, Japan).

Real-Time PCR

Total RNA was isolated from inflamed mucosa of the distal colon 3 cm from the anus, and cDNA was synthesized. Real-time RT-PCR was performed using a Thermal Cycler Dice Real Time System with SYBR Premix Ex TaqII (Takara Bio Inc., Otsu, Shiga, Japan). The primers used were: *Tnfr*, 5'-AACTCGAGTGACAAGCCCGTAG-3' and 5'-GTACCACAGTTGGTTGTCTTTGA-3'; *I11b*, 5'-GCTGTGGCAGC-TACCTATGTCTTG-3' and 5'-AGGTCGTCATCATCCCA-CGAG-3'; *I110*, 5'-CAGACCACATGCTCCGAGA-3' and 5'-CAAGGCTTGGCAACCCAAAGTA-3'; *Ptgs2*, 5'-GCGA-CTGTTCCAAACCAGCA-3' and 5'-TGGGTGCGAACTTG-AGTTTGAAGTG-3'; *Ptges*, 5'-TACGCGGTGGCTGTCA-TCA-3' and 5'-CTCCACATCTGGGTCACTCCTG-3'; *Ppia*, 5'-GGCAAATGCTGGACCAAACAC-3' and 5'-AAACGC-

TCCATGGCTTCCAC-3'. The number of target molecules was normalized against those of *Ppia* as an internal control.²⁰

Reporter Gene Assay of Wnt Signaling

To measure Wnt signaling activity, rat embryonic fibroblasts (REFs) were isolated from E12.5 embryos of F344 and KAD rats in Dulbecco's modified Eagle's medium supplemented with 10% fetal bovine serum. REFs were then plated on 24-well culture plates 24 hours before transfection. Lipofectamine LTX (Invitrogen) was used to co-transfect REFs with pTOPFLASH or pFOPFLASH vector (Millipore, Billerica, MA) and pSV- β -Gal vector (Promega Corp., Madison, WI) as an internal control according to the manufacturer protocol. Cells in half of the plates were stimulated with 150 ng/mL of Wnt3a (R&D Systems Inc., Minneapolis, MN) 3 hours later. Luciferase activities were measured 24 hours after transfection with Luciferase Assay Systems (Promega).

Isolation of VECs

VECs were isolated from the thoracic aorta of four F344 and four KAD rats aged 8 weeks, as described previously.²¹ VECs were cultured in MCDB 131 medium supplemented with epidermal growth factor, endothelial cell growth supplements, vascular endothelial growth factor, hydrocortisone, heparin, and 2% fetal bovine serum. Almost all cultured cells were of endothelial origin, as assessed by staining with Dil-Ac-LDL (Biomedical Technologies Inc., Stoughton, MA). All VECs were examined twice in all *in vitro* experiments to confirm their reproducibility.

Immunofluorescence Microscopy

Cells cultured on collagen-coated coverslips were fixed with 4% paraformaldehyde at 37°C for 15 minutes. After permeabilization and a blocking reaction, they were incubated with antibodies against N-terminal APC (H-290; Santa Cruz), C-terminal APC (C-20; Santa Cruz), α -tubulin (YL1/2; Abcam), paxillin (Abcam), and EB1 (Abcam). They were then treated with Alexa Fluor-conjugated secondary antibodies and phalloidin (Invitrogen), followed by staining with DAPI.

In Vitro Proliferation, Migration, Adhesion, and Tube Formation Assay

A BrdU incorporation assay was performed using the BrdU Labeling and Detection Kit III (Roch Diagnostics GmbH, Mannheim, Germany), according to the manufacturer protocol. Briefly, VECs were plated and labeled with 100 $\mu\text{mol/L}$ BrdU for 6 hours. Cells were stained with the anti-BrdU-POD antibody and quantified by measuring absorbance with an enzyme-linked immunosorbent assay (ELISA) reader. The migration activity of VECs was measured using a wound healing assay, as described

previously.²² Microscopic images were captured at 0 and 16 hours after culture, and the percentage of migrated area was quantified. The adhesion activity of the VECs was measured using a wash assay, as described previously.²³ For tube formation assay, the VECs were plated onto a layer of Matrigel (BD Biosciences, Franklin Lakes, NJ) and incubated at 37°C for 24 hours. Microphotographs of the formation of the capillary-like networks were obtained from at least four fields. Quantitative analyses of their tube length and the number of branching points were performed using WinROOF software version 6.0.

Plasmids

FLAG-tagged rat APC C-terminus (FLAG-APC-C-term), V5-tagged DLG1 and DLG5 plasmids were constructed. Briefly, the coding sequences of rat APC, DLG1, and DLG5 were amplified from brainstem cDNAs of F344/NSlc rats using KOD Plus Neo DNA polymerase (Toyobo, Osaka, Japan). APC C-terminus cDNA (321 amino acids) was cloned into the p3xFLAG-CMV-7.1 vector (Sigma). DLG1 and DLG5 cDNAs were cloned into the pcDNA6.2/V5/GW/D-TOPO vector using a TOPO Expression kit (Invitrogen). To increase efficiency of transfection, the truncated DLG5 cDNAs were cloned. The sequences of PCR primers to amplify the cDNAs are as follows: FLAG-APC-C-term, 5'-CATCTAGCGGCCGCTCAAAGCGGCATGATATCG-CACGCTCCCATCTG-3' and 5'-CTTTCTGGATCCTT-TAAACAGACGTCACGAGGTAAGACCCAGAATGG-3'; DLG1-V5, 5'-CACCATGCCGGTCCGGAAGCAAGATA-CCCAGAGA-3' and 5'-TAATTTTTCTTTTGCTGGGAC-CCAGATGTAAGGACC-3'; DLG5-V5, 5'-CACCATGGA-GCCGAGCGCCGGGAGCTGCTCGCC-3' and 5'-GGG-TGGGCAAGCGGGTATCCACAGGACTTT-3'; DLG5-1-V5, 5'-CACCATGGAGCCGACGCGCCGGGAGCTGCT-CGCC-3' and 5'-TTCCATTTGCTCCTTGAGTTCTTTA-3'; DLG5-2-V5, 5'-CACCTGTGAGCTGGAGAAGGAGGC-3' and 5'-TGAGGTCTGAGGCTGGCTACAGAAG-3'; and DLG5-3-V5, 5'-CACCATGGGCTCTGACAGAGGCTCA-3' and 5'-GGGTGGGCAAGCGGGTATCCACAGGACT-TT-3'. All constructs were verified by sequence analysis.

Co-Immunoprecipitation Assay

A co-immunoprecipitation assay was performed to examine binding reactivity of the C terminus of APC to DLG1 and DLG5. The recombinant V5-tagged rat DLG1 and DLG5 proteins were generated by human cervical cancer cells (Hela cells). Hela cells were cultured in Dulbecco's modified Eagle's medium (Life Technologies, Grand Island, NY) supplemented with 10% fetal bovine serum under an atmosphere of 95% oxygen and 5% carbon dioxide at 37°C. Hela cells were co-transfected with FLAG-APC-C-term plasmids and DLG1-V5, DLG5-V5, DLG5-1-V5, DLG5-2-V5, or DLG5-3-V5 plasmids using Lipofectamine LTX (Invitrogen). As a negative control, p3xFLAG-CMV-7.1 vector

was used. The cells were lysed with Triton X-100 lysis buffer after incubation for 18 hours. The recombinant FLAG-APC-C-term proteins were purified and collected by immunoprecipitation using a FLAG Immunoprecipitation Kit (Sigma). As a positive control, FLAG-BAP fusion protein was used. The resulting supernatants were subjected to immunoblot analysis as described previously.¹⁶ The primary antibodies were rabbit anti-EB1 monoclonal antibody (1:1000, Abcam), mouse anti-V5 monoclonal antibody (1:5000, Invitrogen), and mouse anti-FLAG M2 monoclonal antibody (1:5000, Sigma). The secondary antibodies were

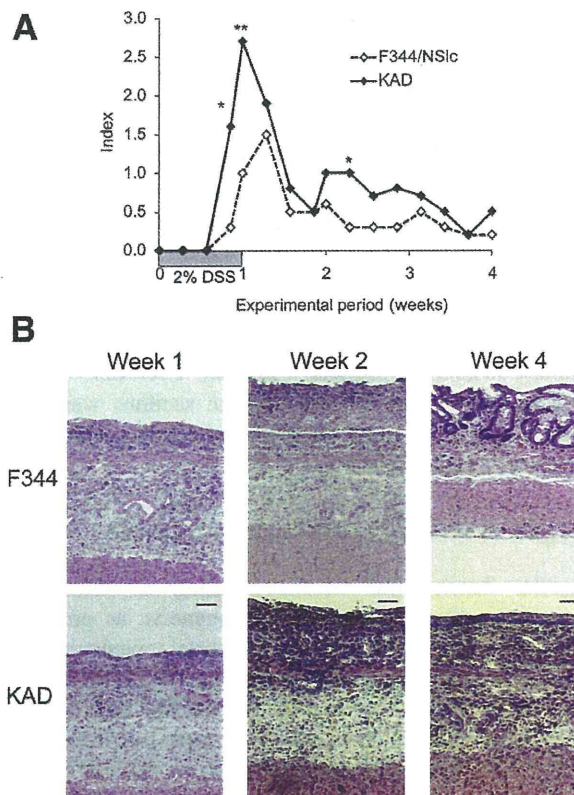


Figure 1 Sustained colon inflammation by DSS in the C terminus of APC-deficient rats. **A:** Clinical inflammatory scores for KAD and F344 rats that received 2% DSS in drinking water. The severity of inflammation was assessed by clinical scoring for diarrhea and fecal blood. * $P < 0.05$, ** $P < 0.02$. **B:** Histologic sections of representative distal colonic lesions of F344 and KAD rats that received drinking water that contained 2% DSS. Pictures were obtained from F344 and KAD rats immediately after terminating DSS exposure (week 1), 1 week after terminating DSS exposure (week 2), and 3 weeks after terminating DSS treatment (week 4). Note mucosal denudation, crypts loss, and diffuse and marked infiltration of inflammatory cells, including polymorph neutrophils, plasma cells, and lymphocytes throughout the lamina propria and submucosa at weeks 1 and 2. At week 1, eosinophilic structures covering the damaged mucosa were observed for F344 but not for KAD rats. At week 4, the mucosal ulcer had healed by crypt degeneration accompanied by fibrosis and a diminished number of inflammatory cells in the F344 rats. However, mucosal ulcers accompanied by diffuse and marked inflammatory cell infiltrate, edema, and dilated small vessels were observed in the lamina propria and submucosa of the distal colon of KAD rats. In some KAD rats, elongation of squamous epithelium was seen on ulcerated mucosa. H&E staining. Original magnification $\times 200$. Scale bar = 100 μ m.

Table 1 Expression Levels of Inflammatory Cytokines in KAD Rats

Gene	Week 0		Week 1		Week 2		Week 4	
	KAD	F344/NSlc	KAD	F344/NSlc	KAD	F344/NSlc	KAD	F344/NSlc
<i>Tnfa</i>	1.26 ± 0.91	1.84 ± 1.53	0.47 ± 1.10	0.25 ± 0.30	88.93 ± 236.33	9.19 ± 11.50	3.24 ± 3.76*	0.22 ± 0.36
<i>Il1β</i>	0.24 ± 0.11	0.49 ± 0.32	118.08 ± 153.51	26.20 ± 33.14	927.33 ± 1204.49	889.79 ± 1233.85	110.61 ± 148.11*	4.70 ± 6.62
<i>Il10</i>	0.02 ± 0.01	0.04 ± 0.03	1.19 ± 1.59	0.26 ± 0.29	2.62 ± 4.37	3.17 ± 2.77	0.65 ± 0.77*	0.05 ± 0.05
<i>Ptgs2/Cox2</i>	0.75 ± 0.37	0.98 ± 0.18	0.34 ± 0.32	0.61 ± 0.77	186.45 ± 344.84	39.82 ± 101.57	13.66 ± 18.92*	0.16 ± 0.23
<i>Ptgs</i>	0.62 ± 0.25	0.44 ± 0.46	13.14 ± 21.22	1.11 ± 1.56	73.20 ± 90.45	58.30 ± 77.77	11.49 ± 12.06*	2.18 ± 2.47

**P* < 0.05.

horseradish peroxidase-conjugated anti-mouse and anti-rabbit IgG (1:2000, Sigma). Immunoblotted proteins were visualized using an ECL select Western blotting detection system (GE Healthcare, Piscataway, NJ).

Statistical Analysis

Student's *t*-test was performed, and SDs were calculated using the statistics package in Microsoft Excel (Microsoft Inc., Redmond, WA). *P* < 0.05 was considered statistically significant.

Results

KAD Rats Display Severe Acute Colitis and Sustained Colonic Inflammation

DSS can effectively induce colonic inflammation in rats, and a loss of body weight, diarrhea, and fecal blood are observed as the clinical symptoms.²⁴ Loss of body weight was noted from day 8 to day 10 in both F344 and KAD rats; however, there were no differences between the two strains of rat. There were no differences in water and food consumption during exposure to DSS (data not shown). KAD rats obtained higher inflammatory scores, mainly resulting from watery diarrhea and visible fecal blood, compared with F344 rats during exposure to DSS. This finding was true even after terminating exposure to DSS (Figure 1A).

Macroscopically, severe inflammation was generally located in the distal colon of the F344 and KAD rats. Prominent macroscopic features of KAD rat colon were dilation, primarily the distal part of the colon (one-third of the colon from the anus), thickening of the colonic wall, and extensive loss of the mucosa accompanied by bleeding. These findings were also observed in F344 rats, but the

Table 2 Labeling Index Observed for DSS-Treated Colonic Mucosa

Week	F344	KAD
2	14.1 ± 7.9	16.1 ± 6.7
4	4.1 ± 1.5	8.5 ± 4.0*

The labeling index was calculated by dividing the number of BrdU-positive cells by the total number of nucleated cells per well-oriented crypt.

**P* < 0.001 compared with F344 rats.

severity was less than that of KAD rats. The changes in KAD rats lasted until week 4; in F344 rats they lasted until week 2, and this was associated with their clinical symptoms.

Histopathologic analysis revealed the presence of mucosal ulceration, crypt loss, diffuse inflammatory cell infiltrate of the lamina propria and submucosa, debris, exudates, edema, and congestion and dilatation of the capillary blood vessels in the affected colons of both F344 and KAD rats at weeks 1 and 2 (Figure 1B). Of note, at week 1, eosinophilic structures covering the damaged mucosa were observed in F344 rats, whereas few structures

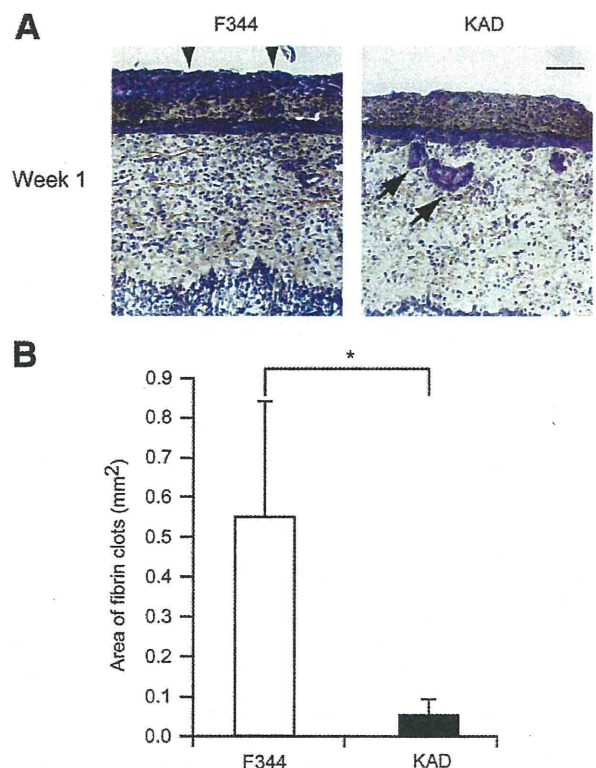


Figure 2 Lack of fibrin clot formation along the mucosal ulcer in the colon of KAD rats. **A:** PTAH-stained sections of F344 and KAD rats at week 1. Fibrin pseudo-membrane covering the surface of the damaged mucosal epithelia was observed in F344 rat colon (arrowheads). Fibrin pseudo-membranes were absent on the colonic mucosa of KAD rats; instead, fibrin microthrombi were observed beneath the lamina propria (arrows). Scale bar = 100 μ m. **B:** The area of fibrin layers covering the surface of DSS-induced inflamed mucosa per rat. **P* < 0.001.

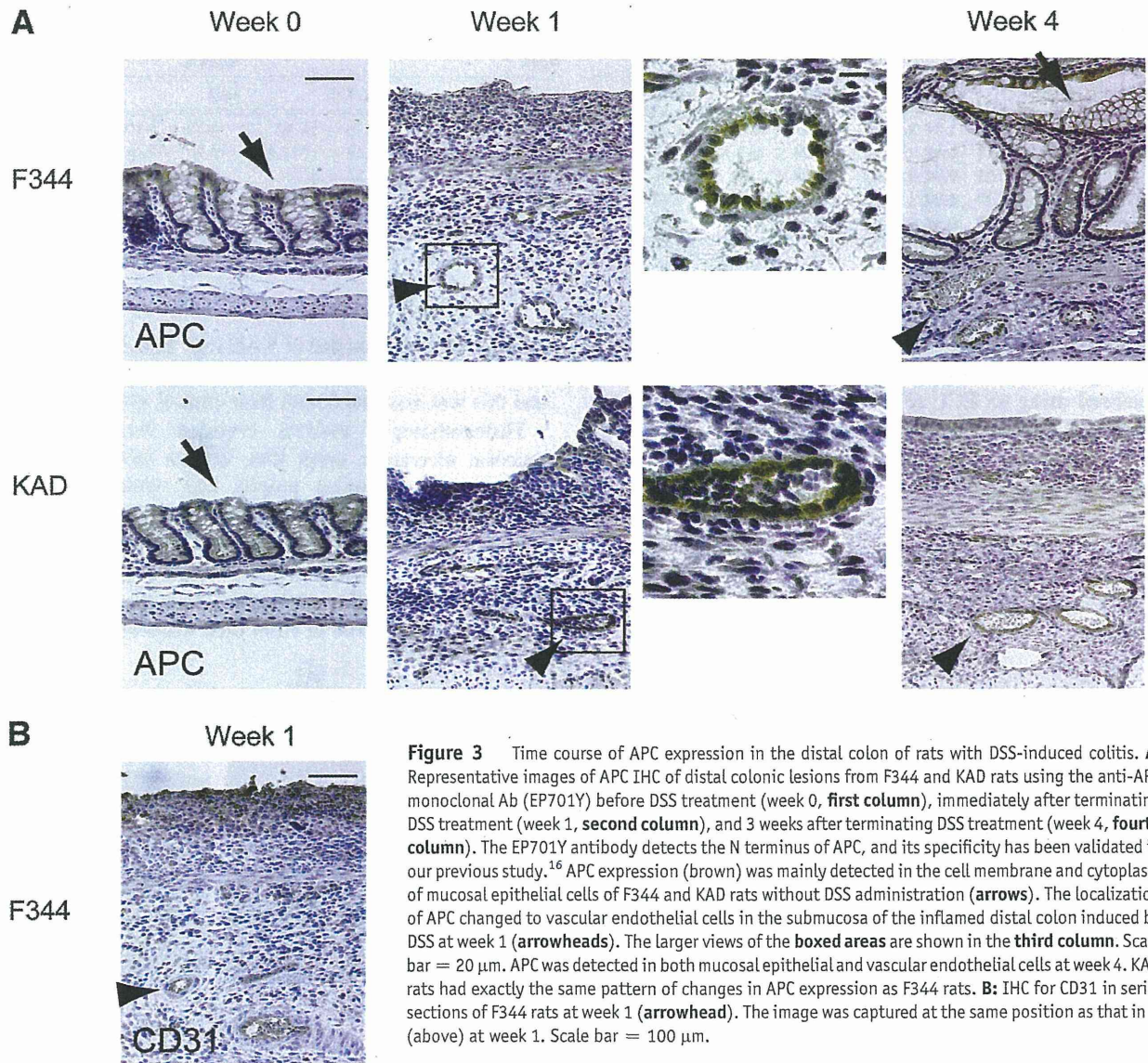


Figure 3 Time course of APC expression in the distal colon of rats with DSS-induced colitis. **A:** Representative images of APC IHC of distal colonic lesions from F344 and KAD rats using the anti-APC monoclonal Ab (EP701Y) before DSS treatment (week 0, **first column**), immediately after terminating DSS treatment (week 1, **second column**), and 3 weeks after terminating DSS treatment (week 4, **fourth column**). The EP701Y antibody detects the N terminus of APC, and its specificity has been validated in our previous study.¹⁶ APC expression (brown) was mainly detected in the cell membrane and cytoplasm of mucosal epithelial cells of F344 and KAD rats without DSS administration (**arrows**). The localization of APC changed to vascular endothelial cells in the submucosa of the inflamed distal colon induced by DSS at week 1 (**arrowheads**). The larger views of the **boxed areas** are shown in the **third column**. Scale bar = 20 μ m. APC was detected in both mucosal epithelial and vascular endothelial cells at week 4. KAD rats had exactly the same pattern of changes in APC expression as F344 rats. **B:** IHC for CD31 in serial sections of F344 rats at week 1 (**arrowhead**). The image was captured at the same position as that in **A** (above) at week 1. Scale bar = 100 μ m.

were observed in KAD rats. Instead, eosinophilic deposits were observed under the lamina propria of KAD rats.

At week 4, the inflammatory changes and mucosal ulcers were resolved for F344 rats, healed by regenerative crypt cells associated with a reduction of the number of inflammatory cells. Severe inflammation was still present in the distal colon of KAD rats, and elongation of the squamous epithelium caused by squamous metaplasia was observed near the border between the rectum and anus. Immune cells, predominantly eosinophilic granulocytes, were continuously observed in the inflamed colon of KAD rats.

Consistent with the histopathologic observations, inflammatory cytokines and mediators, such as *Tnfa*, *Il1 β* , *Ptgs2/Cox2*, and *Ptges*, and the anti-inflammatory cytokine *Il10* were expressed in the inflamed distal colon of DSS-treated KAD and F344 rats (Table 1). The cytokines were most highly expressed at week 2 in KAD and F344

rats. At week 4, the expression of those cytokines decreased in the DSS-treated F344 rat colons. In DSS-treated KAD rat colon, the expression of those cytokines was significantly higher than in F344 rats at week 4. These findings indicate that colitis in KAD rats was remarkably persistent even 3 weeks after termination of DSS treatment.

To assess cell proliferation in the mucosal epithelia, we measured the BrdU-labeling index for the colon epithelia. At week 1, few crypts were observed because of the disrupted architecture of the mucosa or ulceration. Thus, indices could not be calculated. At week 2, the indices were not different between KAD and F344 rats. At week 4, the index for the KAD rats was approximately half of that at week 2 but was significantly higher than that of the F344 rats (Table 2). These findings indicated greater persistence of cell proliferation in the KAD rats compared with the F344 rats at week 4.

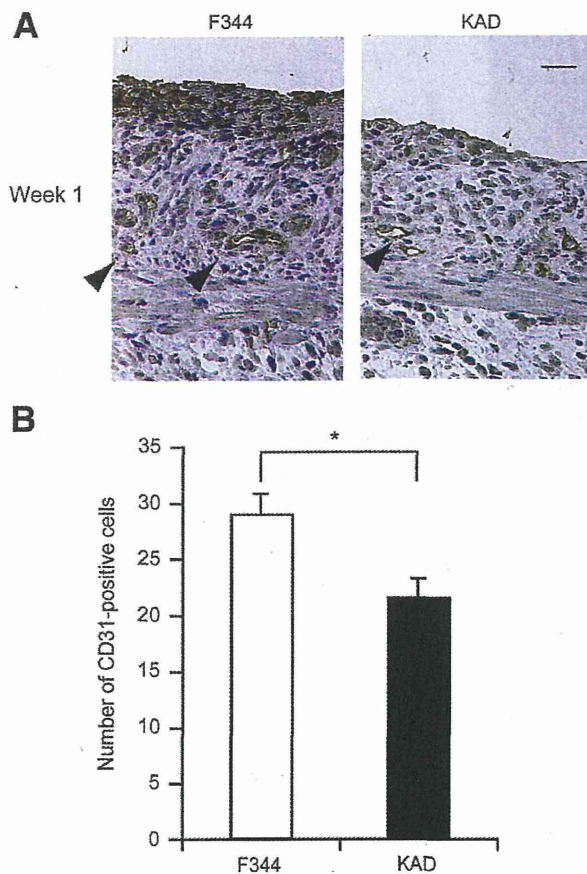


Figure 4 Reduction of angiogenesis associated with an absence of fibrin pseudo-membrane in the DSS-treated colon of KAD rats. **A:** IHC for CD31 of the distal colon of F344 and KAD rats at week 1. CD31-positive cells were clearly present along the ulcerated mucosa of F344 rats, whereas these cells were observed in much smaller numbers in the mucosa of KAD rats (arrowheads). Scale bar = 50 μ m. **B:** Number of CD31-positive cells per field within the mucosa along the inflamed mucosa. * $P < 0.001$.

The Absence of Fibrin Clots along the Damaged Mucosal Epithelia of KAD Rat Colon

To determine whether the eosinophilic structures that had been observed in the colon of F344 rats at week 1 were fibrin clots, we performed PTAH staining on the colonic tissue sections. For F344 rats, fibrin clots formed a pseudo-membrane covering the surface of the inflamed colonic mucosa (Figure 2A). In contrast, for KAD rats, formation of the pseudo-membrane consisting of fibrin clots was much less. Instead, fibrin was deposited mostly in microvessels immediately below the lamina propria and formed microthrombi. The area of the fibrin clots that covered the inflamed mucosa was significantly higher for F344 rats than for KAD rats ($0.56 \pm 0.29 \text{ mm}^2$ versus $0.057 \pm 0.039 \text{ mm}^2$; $P < 0.001$) (Figure 2B). The area of fibrin microthrombi was significantly greater for KAD rats than for F344 rats ($0.060 \pm 0.048 \text{ mm}^2$ versus $0.0047 \pm 0.0050 \text{ mm}^2$; $P < 0.04$). These results indicate that the formation of fibrin layers was defective over the damaged mucosa of KAD rats. Thus, the damaged mucosa of KAD rats

has low potential to form fibrin layers, which make an important contribution to healing the eroded mucosa.

APC Is Expressed in the VECs in the Inflamed Colon

To find a potential association of the presence of APC with colitis, the expression of APC protein was examined in rat colonic tissue. Sequential change of APC expression was generally common in both F344 and KAD rats. At week 0, APC protein was expressed in the cell membrane and cytoplasm of normal mucosal epithelial cells (Figure 3A). At week 1, immediately after DSS treatment, APC protein was highly expressed in VECs in the inflamed submucosa, although no APC could be detected at the mucosal epithelial cells because of their disruption by severe ulceration. At week 4, the expression of APC had recovered in regenerative mucosal epithelial cells and VECs. We confirmed that APC-positive cells in the inflamed distal colon were VECs by immunostaining of serial sections using the anti-CD31 antibody, a positive marker for VECs (Figure 3B). These findings indicate that the expression of APC protein was induced in VECs of the submucosa when colon inflammation occurred.

Reduced Angiogenesis With Inflamed Colonic Mucosa in KAD Rats

Given that APC protein functions in VECs, we examined microvessel angiogenesis in the damaged mucosa by measuring the number of CD31-positive cells in the damaged colonic mucosa at week 1. For F344 rats, many CD31-positive cells were present along the mucosa, which was often associated with the presence of fibrin-like clots (Figure 4A). For KAD rats, fewer CD31-positive cells were observed. The number of microvessels per field along the inflamed mucosa of KAD rats was significantly lower than that of F344 rats (21.70 ± 1.59 versus 29.10 ± 1.83 ; $P < 0.001$) (Figure 4B). These results indicate that microvessel angiogenesis for healing was reduced in the damaged mucosa of KAD rats compared with F344 rats.

Truncated APC of KAD Rats Does Not Affect Wnt Signaling

To clarify whether a loss of the C terminus of APC could affect the regulation of Wnt signaling, we cultured REFs from E12.5 embryos of F344 and KAD rats. We then tested these REFs for their ability to inhibit Tcf-regulated transcription in transfection assays. TOPFLASH luciferase activity in the REFs from F344 and KAD rats was similar to control FOPFLASH activity. Luciferase activity in the REFs of both F344 and KAD rats increased with Wnt3a treatment (Supplemental Figure S1). These results indicate that truncated APC of KAD rats can normally regulate the Tcf-regulated transcription through a Wnt ligand.

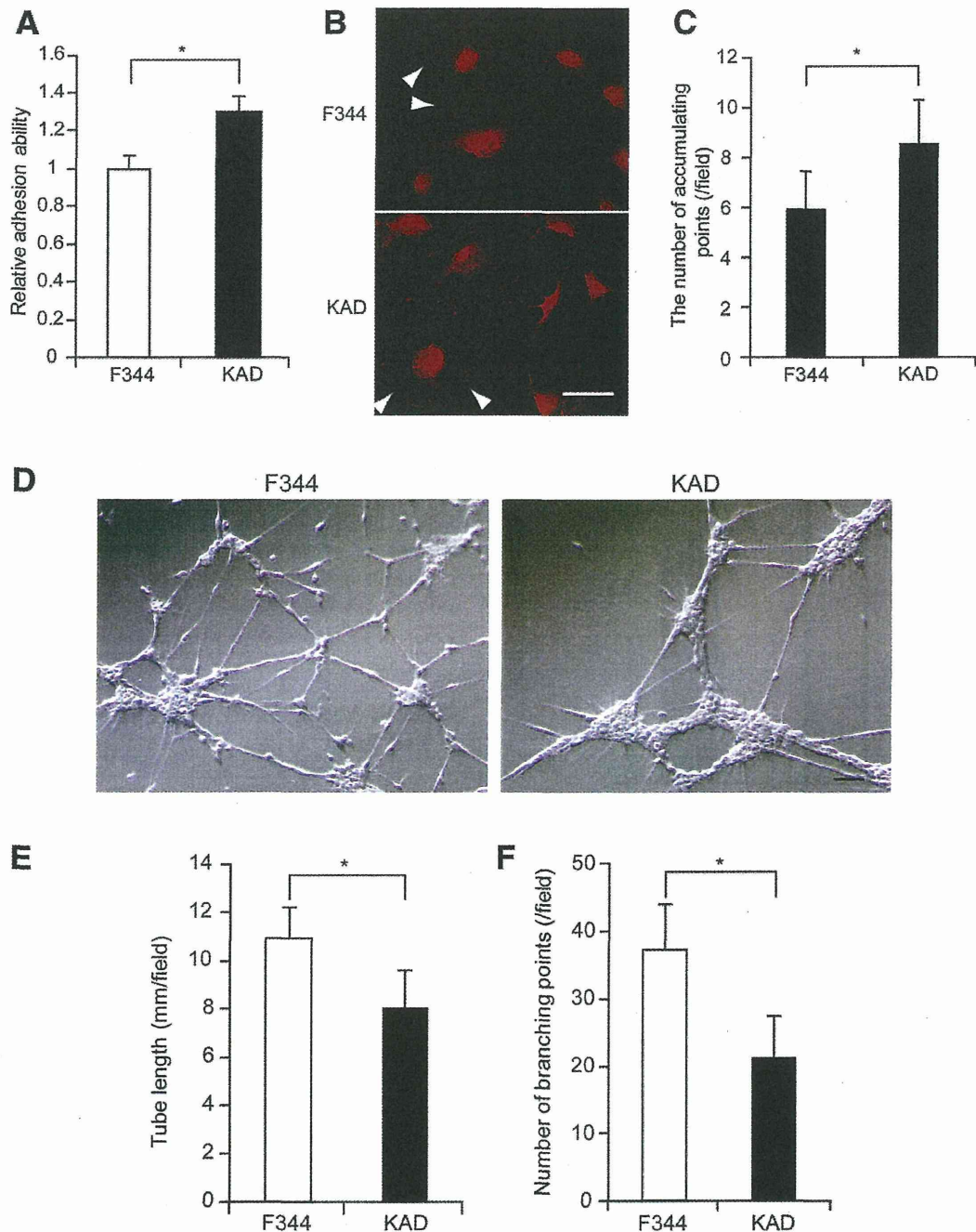


Figure 5 Involvement of APC in endothelial cell tube formation and adhesion. **A:** Wash assay for quantification of adhesion activity of F344 and KAD rat VECs incubated for 30 minutes on collagen-coated wells. Data ($n = 8$) are obtained from two independent experiments. $*P < 0.001$. **B:** Immunofluorescence of paxillin in F344 and KAD rat VECs. Accumulation of paxillin was observed around VECs (arrowheads). Scale bar = 50 μm . **C:** The number of paxillin-accumulating points as focal adhesions in five different areas at the cell periphery was counted in 20 cells. $*P < 0.001$. **D:** VECs isolated from F344 and KAD rats were plated onto Matrigel, and the formation of tube networks were photographed 24 hours after culture. Scale bar = 50 μm . **E and F:** Quantification of tubular length (E) and branching points (F) per field at $\times 100$ magnification. Data ($n = 20$) are obtained from two independent experiments. $*P < 0.001$.

VECs of KAD Rats Show High Adhesion Activity and Abnormal Tube Formation

Migration, adhesion, and polarity of VECs play an essential role in angiogenesis, and their efficiency relies on dynamic rearrangement of the cytoskeleton.^{25,26} To clarify the

involvement of APC in angiogenesis, VECs were isolated from the thoracic aorta of F344 and KAD rats, and their physiologic functions were characterized.

KAD rat VECs had no apparent abnormal morphology when compared with F344 rat VECs and had no difference in the distribution or morphology of either MT or actin

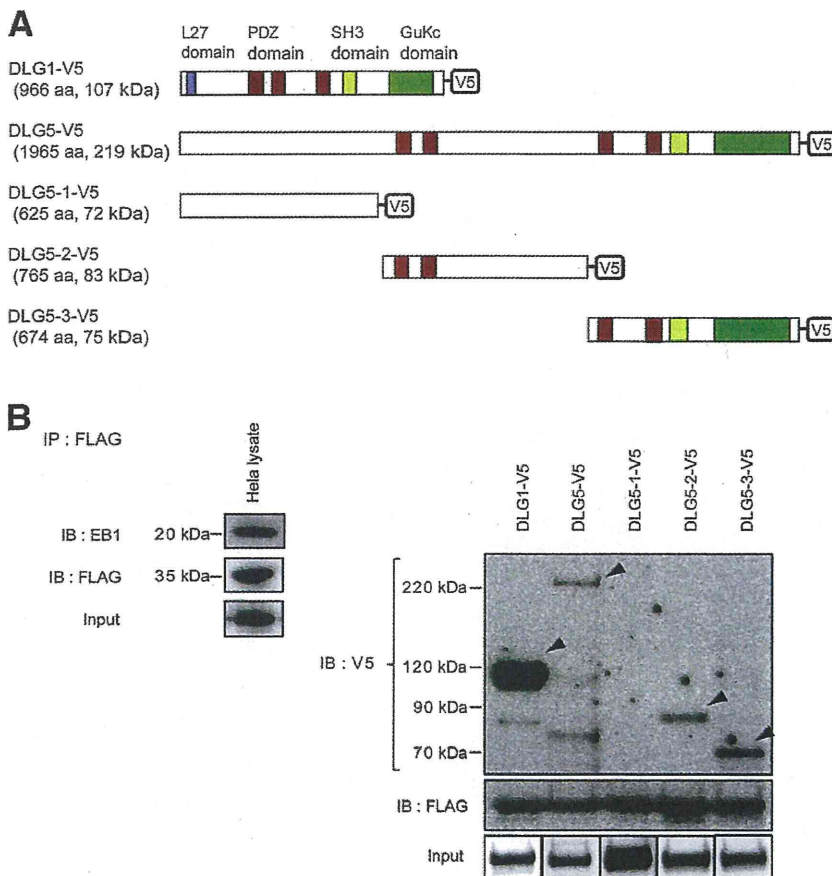


Figure 6 Association of the APC C terminus with EB1, DLG, and DLG5 *in vitro*. **A:** Domain structures and schematic representation of the DLG1 and DLG5 constructs encoding an N-terminal V5 epitope tag: DLG1-V5 (966 amino acids; 107 kDa), DLG5-V5 (1965 amino acids; 219 kDa), DLG5-1-V5 (625 amino acids; 72 kDa), DLG5-2-V5 (765 amino acids; 83 kDa), and DLG5-3-V5 (674 amino acids; 75 kDa). **B:** Binding of the EB1, DLG1, and DLG5 proteins to the FLAG-tagged C terminus of APC (FLAG-APC-C-term; 347 amino acids, 37 kDa) that is absent in the KAD rat. The FLAG-APC-C-term and each construct were co-transfected to HeLa cells. The FLAG-APC-C-term was then immunoprecipitated by the FLAG antibody. Immunoprecipitated proteins were subjected to Western blotting to detect proteins that were co-immunoprecipitated with FLAG-APC-C-term. EB1 was detected using the anti-EB1 antibody. DLG1, DLG5, DLG5-1, DLG5-2, and DLG5-3 were detected using the anti-V5 antibody. EB1, DLG1, DLG5, DLG5-2, and DLG5-3 were co-immunoprecipitated with the FLAG-APC-C-term (arrowheads).

cytoskeleton. APC protein accumulated at the ends of the MTs at the migrating edges of both F344 and KAD rat VECs (Supplemental Figure S2). The incorporation of BrdU into KAD rat VECs was not different from that seen in F344 rat VECs (F344: 1.00 ± 0.04 versus KAD: 1.01 ± 0.03 ; $P = 0.92$). A wound healing assay demonstrated that the migration activity of KAD rat VECs stimulated with vascular endothelial growth factor was not different from that of F344 rat VECs (F344: 44.9 ± 6.03 versus KAD: 41.7 ± 7.30 ; $P = 0.11$).

A wash assay revealed significantly higher adhesion activity in KAD rat VECs than that in F344 rat VECs (Figure 5A). Immunostaining with antipaxillin antibody demonstrated that the number of focal adhesion sites of KAD rat VECs was significantly higher than that of F344 rat VECs (Figure 5, B and C). The capillary-like structure of KAD rat VECs induced on Matrigel revealed apparent differences in morphology compared with those of F344 rat VECs (Figure 5D). The length of tubes of KAD rat VECs was significantly shorter than that of F344 rat VECs (Figure 5E). The number of branches of KAD rat VECs was significantly fewer than that of F344 rat VECs (Figure 5F). These findings indicate that KAD rat VECs had normal physiologic function in morphology, proliferation, and migration but defects in adhesion and tube formation.

EB1 and DLG5 Could Bind to the C Terminus of APC and Are Expressed in the VECs of the Inflamed Colonic Region

To find molecules that interact with the C terminus of APC at the VEC in the inflamed area, we performed an Immunoprecipitation assay and fluorescent IHC. The C terminus of APC, which is absent in KAD rats, can interact with EB1 and DLG1.¹² Recently, DLG5 has been reported to be associated with pathogenesis of IBD.²⁷ Because DLG5 and DLG1 share the postsynaptic density protein-95/disks large/zonula occludens-1 (PDZ) domains that are known to bind to the C terminus of APC (Figure 6A) and the most characteristic feature of IBD is sustained inflammation of the colon, we examined whether DLG5, similar to EB1 and DLG1, can bind to the C terminus of APC.

Similar to EB1 and DLG1, full-length DLG5 was co-immunoprecipitated with the FLAG-APC-C-term (Figure 6B). Although we could not detect DLG5-1-V5, containing the first third of DLG5, we could detect DLG5-2-V5 and DLG5-3-V5, containing the second and final third of DLG5, respectively (Figure 6B). Both DLG5-2-V5 and DLG5-3-V5 contain PDZ domains, similar to DLG1, but the DLG-1-V5 contained no PDZ domain. Thus, these results indicate that the C terminus of APC could interact with the PDZ domain of DLG5.